J Therm Anal Calorim (2011) 105:229–238
DOI 10.1007/s10973-011-1365-4

Growth and thermal kinetics of pure and cadmium doped barium phosphate single crystal

Shivani Suri · K. K. Bamzai · Vishal Singh

Received: 9 November 2010 / Accepted: 20 January 2011 / Published online: 15 February 2011

Abstract Non-isothermal kinetic parameter of pure and cadmium-doped barium phosphate single crystal grown by room temperature solution technique have been investigated. Single crystal X-ray diffraction establishes grown crystal to be orthorhombic in nature. Scanning electron microscopy supplemented with energy dispersive X-ray analysis was used to study the surface features and to find the exact stoichiometric composition of the grown crystal. Fourier transform infrared spectroscopy studies confirm the presence of various functional groups. The effect of cadmium doping on pure barium phosphate single crystal was studied using thermogravimetry analysis. Thermogravimetry studies shows that the pure crystal was stable up to a temperature of 330 °C whereas doped crystal was stable up to a temperature of 240 °C, i.e., pure crystals were more stable than doped ones. Various solid-state reaction kinetics, i.e., activation energy (E_a), frequency factor (Z), and entropy (ΔS^*) was calculated out to find the mechanism of thermal decomposition at different stages for pure and cadmium doped barium phosphate.

Keywords Transition metal compound · Crystal growth · Phase transitions thermogravimety · Differential thermal analysis · Differential scanning calorimetry

Introduction

Phosphate crystals are regarded as technically very potential materials. Phosphates represent the most interesting class of new inorganic phosphate owing to the adaptability of the PO_4 tetrahedron in bonding to other diverse structural units. Inorganic phosphate includes large number of diverse materials that find their utility in the wide range of applications including catalysts, linear and non-linear optical components, solid electrolytes for batteries, etc. They have attracted more and more interest on synthesis, crystallography and electro-optical materials, and so on [1, 2]. Among the various phosphate crystals, potassium di-hydrogen phosphate (KDP) is one of the best known ferroelectric materials. KDP belongs to family of crystals that exhibit excellent quadratic non-linearity. KDP crystal is well known for their good piezoelectric and non-linear optical properties, which have drawn much attention for their significant theoretical interests and commercial applications in the optical modulation, frequency conversions, electro- optics, and so on [3, 4].

In recent decade, the topic of crystal growth has developed from being a largely academic discipline to being one of the key fields in material science. Several researchers have grown materials in the form of single crystal by gel technique. The gel growth technique appeared to be quiet attractive for growing crystals of group II compound on account of its unique advantages in terms of crystals produced and simplicity of the process [5–7]. The alkaline earth phosphates have received enormous importance with respect to their use as phosphor matrices [8]. Several researchers have used gel technique to grow single crystals and also modified them by suitable substitution to determine the effect of modification on their substitution. The effect of doping on gel grown crystals has been studied by Dishovshy and Mladenova [9] and Dennis and Henisch [10]. The effect of chromium doping on the crystalline quality of ammonium hydrogen phosphate (ADP) has been studied by Gits et al. [11]. Recently, a few

S. Suri · K. K. Bamzai (✉) · V. Singh
Department of Physics and Electronics, Crystal Growth and Materials Research Laboratory, University of Jammu, Jammu 180006, India
e-mail: kkbamz@yahoo.com

reports have been published concerning the growth of doped crystal employing gel technique, these include crystals of strontium chromium magnesium hydrogen phosphate (SrCrMHP) [12] and strontium calcium magnesium hydrogen phosphate (SrCaMHP) [13]. There are some reports of crystallization and thermal characteristics of calcium hydrogen phosphate dihydrate crystals [14, 15]. Thermal characteristics of rare earth doped calcium hydrogen phosphate single crystals [16] as well as synthesis and characterization of some rare earth phosphate fibrous have been also investigated by various workers [17–20]. Thus, the effect of dopants on various properties of single crystals is of great interest from both solid-state science and technological point of view [21, 22]. There are also a few reports, which provide information regarding growth and characterization of barium hydrogen phosphate crystals [23, 24].

In this article, authors report the growth and thermal kinetics of pure and cadmium (Cd) doped barium (Ba) phosphate crystals by room temperature solution technique. The substituted ion that have been selected for modified barium phosphate is Cd, because the ionic radii of Cd ion (0.97 Å) is close to that of Ba ion (1.35 Å) in comparison to the other elements (oxygen and phosphorus) present in the grown composition. Therefore, author reports for the first time characterization and non-isothermal kinetics of barium phosphate, which is thermally stable up to 330 °C instead of already, reported barium hydrogen phosphate which is thermally stable only up to 120 °C [25].

Experimental technique

Room temperature solution technique known as gel technique is used for the growth of both pure and Cd doped barium phosphate single crystals. The crystallization apparatus used for the growth purposes consists of borosilicate glass tube of length 20 cm and diameter 2.5 cm. The reactants used for the growth of pure crystals in silica gel are orthophosphoric acid as the lower reactant and barium chloride as the upper reactant. In order to grow crystals from silica gel, first of all silica gel solution of desired molarity is prepared by dissolving sodium metasilicate powder in distilled water. The sodium metasilicate solution is then impregnated with orthophosphoric acid in accordance with desired pH value with continuous stirring in order to avoid any local ion concentration which would other wise caused premature local gelling and make final solution inhomogeneous. The pH value of the solution is adjusted in the value ranging from 4 to 7. A gel solution of fix amount with desired pH value is then allowed to set in the crystallizer in the form of test tube. The gel setting time is found to be strongly pH dependent and environmental temperature. It may take about 24 h for the gel to set in summer (35–40 °C) whereas in winter (10–15 °C) it would take even 14 days for the gel to set. After gel setting, an aqueous solution of barium chloride ($BaCl_2$) of particular molarity is poured over the gel carefully along the walls of the test tube so as to avoid any gel breakage. The following reaction is expected to take place leading to the formation of barium phosphate crystals.

$$BaCl_2 + H_3PO_4 \rightarrow Ba_3(PO_4)_2 + 6HCl$$

Similarly, for the growth of Cd-doped barium phosphate crystals, lower reactant remains the same. However, for upper reactant a mixture of Cd chloride and barium chloride solution in proper ratio is used. Here, $BaCl_2$ solution is first mixed with an aqueous solution of Cd chloride ($CdCl_2$) of particular molarity and then this mixed solution is poured over the gel carefully along the walls of the test tube. The diffusion of Ba^{2+} and Cd^{2+} ions through the narrow pores of the silica gel leads to the reaction between these ions and H_3PO_4 ions present in the gel as lower reactant. The reaction leads to the formation of Cd-doped barium phosphate crystals.

Characterization technique

The morphology of the grown crystals was studied using scanning electron microscope (SEM, Model JEOL 840). Single crystal X-ray diffraction study was carried out using single crystal Oxford X-ray diffractometer, whereas the powder pattern was obtained using powder X-ray diffractometer (Rigaku Co. Ltd. Japan) with Cu K_α radiation ($\lambda = 1.54$ Å) with a scanning rate of 2°/min. Energy dispersive X-rays analysis (EDAX) was recorded using dispersive spectrometer (INCA ENERGY EDAX) attached to the scanning electron microscope for carrying out elemental analysis of the grown crystals. The Fourier transform infrared (FTIR) spectra was recorded in the wave number range of 4000–400 cm^{-1} by the Perkin-Elmer 781 spectrophotometer using KBr pellet method. The thermal behavior of the material was investigated using thermogravimetric (TG), differential thermal analysis (DTA), and differential scanning calorimetry (DSC). TG and DTA curves were recorded simultaneously by a thermal analyzer (Shimadzu make DTG-60) over the temperature range from 25 to 1000 °C in the N_2 atmosphere at a heating rate of 15 °C/min and flow rate of 30 mL/min. The DSC measurements were carried out on a DSC thermal analyzer (DSC-60 Shimadzu make) over a temperature range from 25 to 500 °C in the Nitrogen (N_2) atmosphere at a heating rate of 15 °C/min and flow rate of 30 mL/min. Based on thermal analysis results, solid state reaction kinetic studies were carried out using non-isothermal kinetic parameters.

Results and discussion

Crystal growth

In order to establish the conditions conducive for the growth of barium phosphate (BP) and Cd doped barium phosphate (CdBP) in the form of single crystals, number of experiments were performed under varying conditions of different growth parameters viz., gel pH, concentration of upper and lower reactant, gel aging, and gel molarity. Once the upper reactant of desired molarity was poured on a perfectly set gel, then nucleation starts and the anions of barium chloride slowly diffused into the gel column containing phosphate ions and react together to form the expected crystals, which start appearing in the crystallizer as shown in the Fig. 1. This figure shows the growth of pure BP crystals in a crystallizer. The fully grown crystals were then removed from the crystallizing tube while washing in distilled water. The crystals were then dried and placed in the vacuum so that they do not come in contact with dust particles. Some of the good quality crystals of pure BP of the order of 4–5 mm in size is shown in Fig. 2. After series of experiments optimum conditions for the growth of good quality BP crystals are: lower reactant: 0.5 M, upper reactant: 0.5 M, gel concentration: 0.5 M, gel aging: 96 h, gel pH: 6, and growth temperature: 30 °C. Similar parameters were obtained for the growth of good quality CdBP crystals.

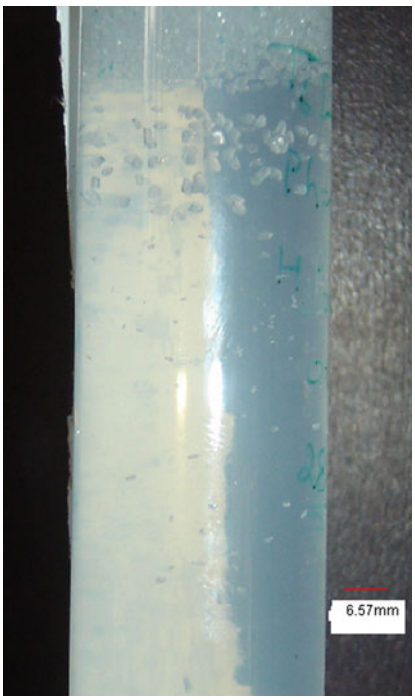

Fig. 1 Growth of BP crystals in a crystallizer

Fig. 2 Different sized crystals of BP placed on micro slide

Scanning electron microscopy (SEM)

In order to study the surface features of the grown crystal, scanning electron microscopic studies of both BP and CdBP crystals were performed. Figure 3a shows different type of morphologies exhibited by pure BP crystals as seen under scanning electron microscope. The various types of morphologies include spherulites, platelets, cuboids, and coalesced crystals. Figure 3b shows the feature of same crystal under scanning electron microscope at higher magnification showing crystal surface along with some gel inclusions, which means that crystals were not properly cleaned while taking out from the crystallizer.

X-ray diffraction analysis (XRD)

The powder X-ray diffractograms for both BP and CdBP crystal is shown in Fig. 4. The crystallinity of both the grown crystals is quiet clear from diffractograms because of the occurrence of sharp peaks at a specific 2θ Bragg angles. From the diffractogram, it is clear that the entry of the Cd ions in the modified composition of BP crystals lead to shift in the positions of peaks which shows that doping has brought about a change in the internal structure of crystals due to the change in bond lengths. Thus, it has been observed that because of Cd doping peak value shifts toward higher angle, indicating a decrease in the value of lattice constants**.** The details of the XRD plot depicting 'd' spacing and corresponding [hkl] planes for pure and doped one is given in the Table 1. Single crystal X-ray establishes that BP and a CdBP crystal belongs to orthorhombic crystal system as has been obtained in case of barium hydrogen phosphate crystal [24]. The lattice parameters obtained in case of pure are: a = 4.60, b = 14.10, c = 17.16 Å and

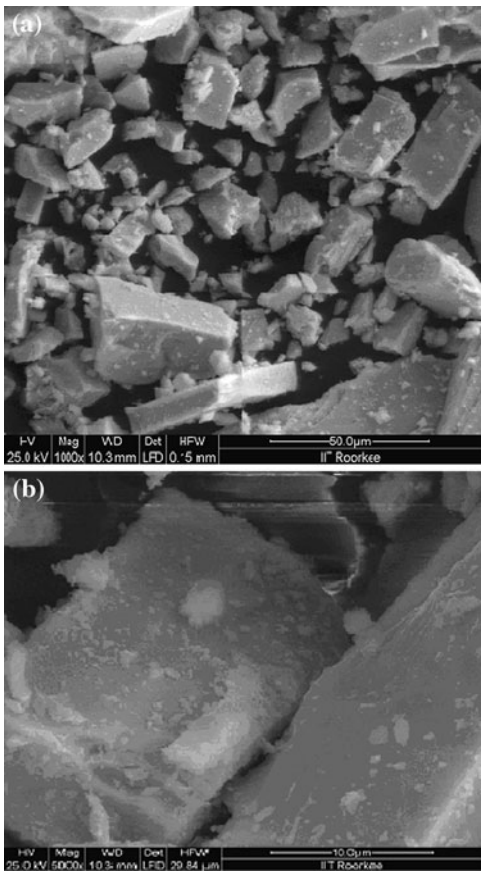

Fig. 3 Electron micrograph showing **a** BP crystals having different morphologies; **b** a portion of BP crystal taken at higher magnification revealing the growth of crystals along with gel inclusions

$\alpha = 90.00°$, $\beta = 90.02$, $\gamma = 90.00°$ with space group Pnma and volume of unit cell being 1082.45 Å. Similarly, the lattice parameters obtained in case of doped crystals are: a = 4.59, b = 14.05, c = 17.10 Å and $\alpha = 90°$, $\beta = 90.01°$, $\gamma = 90.15°$ with space group Pmma and volume of unit cell being 1107.70 Å. From the powder as well as single crystal XRD data it has been found that BP and CdBP crystals belongs to orthorhombic crystal system. Thus, the doping of Cd into BP does not change the crystal system of the BP. From the experiments performed, it has been found that the maximum amount of Cd doping which does not change the crystal structure is about 30%.

Energy dispersive X-ray analysis (EDAX)

EDAX is a technique, which makes it possible to identify elements and know their concentration by analyzing the energies of X-ray photons emitted as a result of bombardment by an electron beam. The spectrum obtained from EDAX analysis for pure and doped is shown in Fig. 5. EDAX pattern shows peaks corresponding to all the major

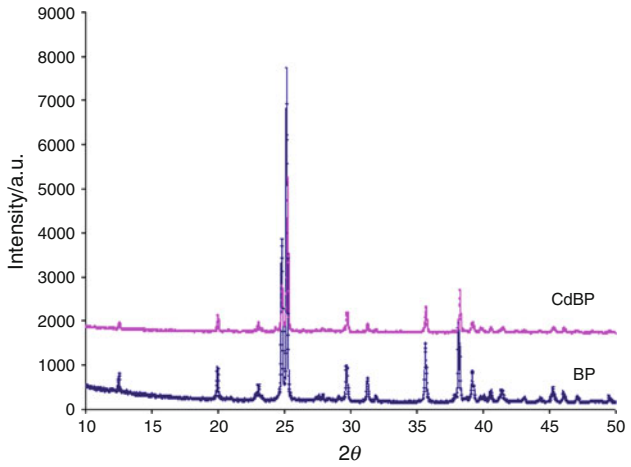

Fig. 4 X-ray diffraction of BP and CdBP showing well-defined Bragg peaks at 2θ angles

Table 1 Compiled data of various hkl planes corresponding to different Bragg angle and inter planer spacing for BP and CdBP

d-Spacing/Å		$2\theta/\theta$		[hkl] Planes		Intensity/counts	
BP	CdBP	BP	CdBP	BP	CdBP	BP	CdBP
7.04	7.024	12.54	12.59	020	020	343	169
4.44	4.43	19.96	20.02	101	023	633	352
3.85	3.83	23.02	23.15	120	120	356	218
3.58	3.57	24.82	24.83	103	103	2794	956
3.52	3.51	25.26	25.33	122	040	6734	3557
3.00	2.99	29.69	29.83	043	043	725	450
2.85	2.85	31.27	31.36	133	006	475	211
2.52	2.52	35.59	35.56	143	053	1002	513
2.36	2.35	38.08	38.26	054	054	1239	724
2.29	2.29	39.21	39.22	200	200	580	260

elements present in the grown crystal as should be expected from pure crystals. The spectra corresponding to CdBP crystals shows peaks corresponding to all major elements along with Cd thereby suggesting that Cd^{2+} ion has entered into the crystal lattice of the BP. However, in case of BP, along with the expected elements some trace impurities in the form of chlorine and nitrogen are also observed. The experimental and theoretical calculated atomic and weight percentage of elements in pure and Cd doped crystals is given in the Table 2a, b, respectively. For BP, theoretical values are calculated as per the formula $Ba_3(PO_4)_2{\cdot}H_2O$ whereas for CdBP, the values are calculated as per the formula $Cd_{3(0.1)}Ba_{3(0.9)}(PO_4)_2{\cdot}H_2O$. The experimental and theoretical values are in close agreement with each other. The above composition and presence of water molecules in pure and doped crystals gets further confirmed by FTIR and thermoanalytical analysis.

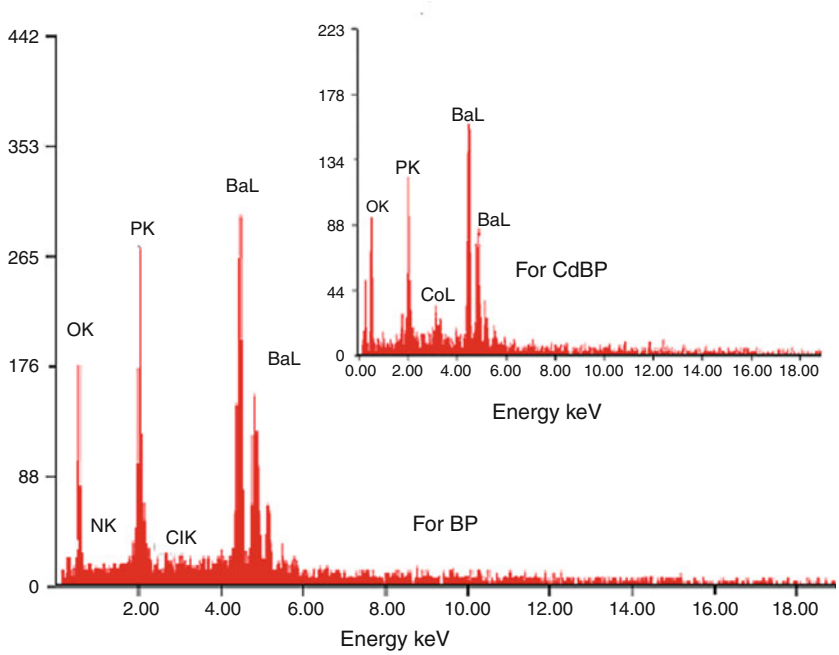

Fig. 5 Energy dispersive X-ray analysis (EDAX) spectrum revealing the presence of major element in the BP crystal, whereas spectrum for CdBP crystal is shown in the *inset*

Table 2 Experimental and theoretical calculated composition obtained from energy dispersive X-ray analysis (EDAX) of various constituent elements present

Element	Experimental values		Theoretical calculated values	
	Wt/%	At/%	Wt/%	At/%
(a) In case of barium phosphate (BP)				
Oxygen	20.59	53.83	22.65	59.5
Phosphorus	14.75	19.91	9.74	13.22
Barium	61.91	18.85	64.85	19.84
(b) In case of cadmium doped barium phosphate (CdBP)				
Oxygen	20.78	58.64	23.57	64.28
Phosphorus	13.11	19.11	10.14	14.28
Barium	58.97	19.39	60.75	19.28
Cadmium	07.14	02.87	05.51	2.14

Fourier transform infrared spectroscopy (FTIR)

FTIR spectrum recorded for pure BP and CdBP crystal is shown in Fig. 6a, b, respectively. Fundamental IR frequencies observed in all other phosphate compounds, are also found in the present case, which confirms the presence of phosphate group in the grown crystals. A comparison of the bands and peaks of the FTIR spectra for pure and doped reveal interesting features. The presence of band at 3431.6 cm^{-1} for pure and 3482 cm^{-1} for Cd doped indicates the presence of water of hydration in both the crystals. The peaks corresponding to other functional groups are also present in both the cases. As seen from the spectrum, a slight shift is observed in some of the characteristically vibrational frequency in case of CdBP with respect to BP because of Cd doping. It could be due to the lattice strain developed as a result of doping. The shift in the wave number was due to the difference in mass number of Cd (112.40) and barium (137.34) ions. It is reported in the literature [26], that the difference in mass of ions leads to a change in the molecular geometry and mechanical vibrations, which results in a shift in bands. A comparative assignment of prominent peaks of FTIR spectra is given in the Table 3.

Thermal analysis

The analysis of recorded curve is quiet helpful in determining the thermal stability, composition and solid-state kinetics of dissociation of the grown material. Figure 7a gives simultaneously recorded TG and DTA curve for BP crystal. From the curve, it is clear that when the material is heated at uniform rate, it loses weight as a continuous function of temperature. The thermal stability of the grown material can be explained in two steps. The curve shows that the material (BP) is thermally stable up to a temperature of 330 °C and thereafter it start decomposing whereas barium hydrogen phosphate (BHP) crystal already reported [25] is thermally stable up to a temperature of 120 °C. The first stage of decomposition begins from 330 °C and continues up to a temperature of 394 °C resulting in a weight loss of 3.71%. This weight loss is attributed to the loss of one water molecule from the grown material. The second stage of decomposition starts from 394 °C and ends at 480 °C, leading to weight loss of 20.92%. During the second stage of decomposition, abrupt weight loss occurs which corresponds to the conversion of anhydrous BP into

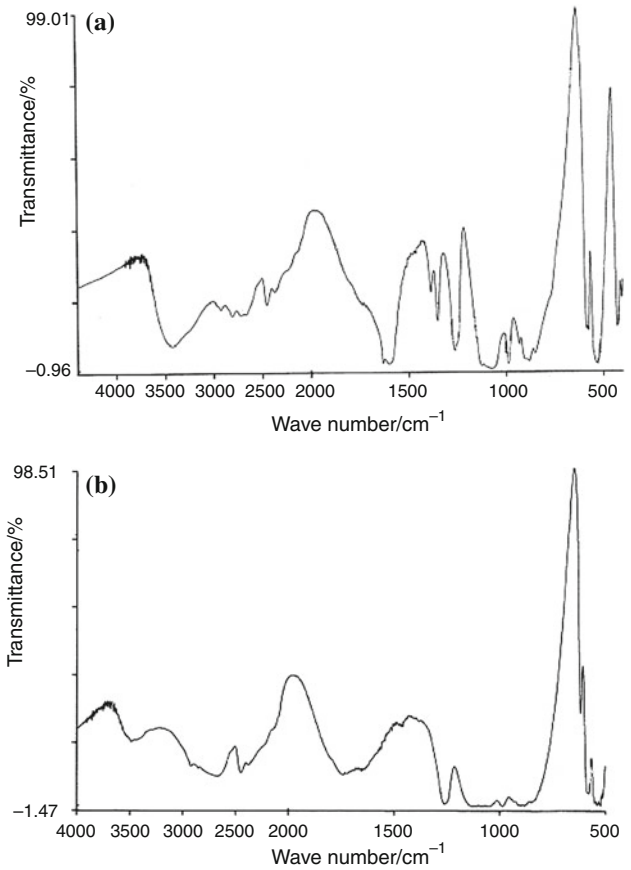

Fig. 6 Fourier transform infrared spectroscopy (FTIR) spectrum of the crystal depicting the various functional groups present in **a** BP; **b** CdBP

Table 3 Presence of various functional groups in case of pure BP and CdBP crystals

Assignments of bands/peaks	Peaks for BP	Peaks for CdBP
O–H symmetric and asymmetric stretching	3431.5	3482.5
Si–H bond	2381.9	2449.6
H–O–H bending	1598.1	1457.5
P=O stretching	1262	1261
P–O stretching	987.3, 880.1	984.1, 881.8
P–P stretching	578.4	577.5
Metal-oxy bond	530.4, 429.2, 405.5	522.3

metal oxide there by liberating P_2O_5 (gas) ion. Thus, there is a change in thermodynamic system from one phase to another as a result of changing temperature which is known as phase transition. In general, first order phase transitions are those where first order partial derivative of the free energy with thermodynamical variables, e.g., pressure, temperature exhibit discontinuities. These first order derivatives can be volume, entropy, and enthalpy. Hence melting, evaporation, sublimation, crystal to crystal transition, crystallization, condensation, depositions all are the first order phase transitions. In this case, as there is an evaporation/liberation of P_2O_5 (gas) ion, there by suggesting that the transition in the crystal system belongs to first order phase transition. After the second stage of decomposition, the material is thermally stable up to the end of the analysis. It can be seen that the calculated weight losses are in close proximity with the observed values. Based on these thermal analyses, the authors can further confirm that the grown crystal is having a composition of $Ba_3\ (PO_4)_2{\cdot}H_2O$.

Figure 7b shows the simultaneously recorded TG and DTA curve for CdBP crystals. From the curve, it is clear that doped crystals are thermally stable up to temperature of 240 °C and thereafter they start decomposing. This means that pure crystals are more stable than doped ones. The whole decomposition process takes place in two steps. The first stage of decomposition starts from 240 °C and continues up to a temperature of 251 °C resulting in a weight loss of 2.30% and thereafter it remains stable in the temperature range of 251–332 °C. After this temperature, it loses weight and dissociation of the material takes place in temperature range of 332–505 °C leading to a weight loss of 16.07%. Table 4b gives detailed summary of the decomposition of $Cd_{3(0.1)}Ba_{3(0.9)}(PO_4)_2{\cdot}H_2O$ along with observed as well as calculated weight loss. In this case also, the calculated and observed weight loss is in close agreement with each other. It is worth mentioning here that the temperature for the formation of stable product after decomposition in case of pure one is 480 °C whereas in case of doped one is 505 °C. This means that the temperature for the formation of end product increases with Cd substitution. Also pure crystals are more stable than doped ones.

As seen from DTA curve in case of BP and CdBP crystals (Fig. 7a, b), there are well-marked endothermic and exothermic peaks corresponding to each stage of decomposition. Since peaks in DTA curve corresponds to weight loss in TG curve thereby suggesting some structural changes taking place besides certain weight loss. The existence of these peaks can be explained in terms of energy requirements. The energy of peaks does not necessarily depend only on the amount of water loss on dehydration but also depends on the structural factors.

DSC plot of BP and CdBP is shown in Fig. 8a, b, respectively. It was the limitation on the part of the DSC instrument that the authors cannot go beyond 500 °C. The peaks in the DSC plot, indicates all transformations taking place in the material up to 500 °C. The peak at 427 °C for BP nearly coincides with the DTA peak at 450 °C. Shift in the temperature is expected in the results because of the instrumental error. The enthalpy value corresponding to endothermic peak in DSC plot is −121 mJ or –23.24 J/g.

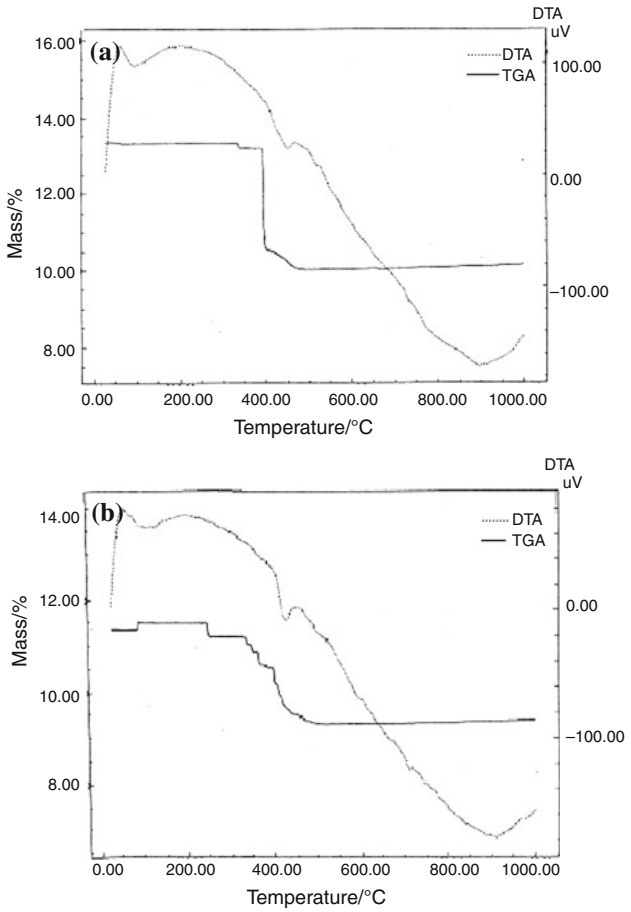

Fig. 7 Curve showing simultaneous recording of thermogravimetry (TG) and differential thermal analysis (DTA) curves for **a** BP; **b** CdBP

In case of CdBP, peak at 443 °C in DSC curve coincide with DTA peak at 425 °C. The enthalpy value corresponding to endothermic peak in DSC plot is –89.85 mJ or –11.82 J/g. The change in the enthalpy value also suggests the transitions taking place in the system belonging to first order in both BP and CdBP crystals. From the above discussion one can suggest that the maximum temperature limit for working with pure BP crystal is 330 °C whereas for CdBP crystals the limit is 240 °C.

Non-isothermal kinetic parameters of thermal analysis

For the determination of kinetic parameters in a solid-state decomposition reaction, data is usually obtained at different temperatures. Also different models have been proposed depending on the type of process leading to the reaction [27]. In this study, three equations viz., Horowitz–Metzger [28], Coats–Redfern [29], and Piloyan et al. [30] were used for calculating energy of activation (E_a), order of reaction (n), frequency factor (Z) and entropy (ΔS^*). The kinetics is studied for both pure (BP) as well as doped (CdBP) crystals for the two stages of decomposition.

Horowitz–Metzger relation

Horowitz–Metzger relation gave a sufficiently accurate and convenient method of modeling. Horowitz–Metzger equation is given by the relation:

$$\log[g(\alpha)] = \log[-\ln(1-\alpha)] = E_a\theta/2.303RT_m^2 \quad \text{for } n = 1$$

$$\log[g(\alpha)] = \log\left[1-(1-\alpha)^{1-n}/1-n\right] = E_a\theta/2.303RT_m^2 \quad \text{for } n \neq 1$$

i.e., $n = 1/2, 1/4, 2/3, 1/3$

In this relation, α denote the fractional mass loss. The value of 'α' is equal to the total mass loss up to a particular temperature divided by mass loss in the step involved, 'n' is the order of reaction and 'R' is the gas constant. $\theta = T - T_m$, where T_m is the temperature of maximum reaction rate and T is the temperature in Kelvin at any instant. A graph of log [g (α)] against θ shows linear dependence, from the slope of which activation energy (E_a) is calculated. In order to obtain the best linear fit for the model proposed for the mechanism of decomposition of the material, the order of reaction (n) is taken as ½.

Table 4 Results of thermal decomposition for different temperature ranges with observed and calculated weight loss

Stage	Temperature/°C	Decomposition step	Weight loss/%	
			Obs.	Cal.
(a) In case of barium phosphate (BP)				
I	330–394	$Ba_3(PO_4)_2{\cdot}H_2O \rightarrow Ba_3(PO_4)_2 + H_2O$	3.71	2.83
II	394–480	$Ba_3(PO_4)_2 \rightarrow 3BaO + P_2O_5$	20.92	22.96
(b) In case of cadmium doped barium phosphate (CdBP)				
I	240–251	$Cd_{3\ (0.1)}Ba_{3\ (0.9)}(PO_4)_2{\cdot}H_2O \rightarrow Cd_{3\ (0.1)}Ba_{3\ (0.9)}(PO_4)_2 + H_2O$	2.3	2.8
II	332–505	$Cd_{3\ (0.1)}Ba_{3\ (0.9)}(PO_4)_2 \rightarrow Cd_{3\ (0.1)}Ba_{3\ (0.9)}PO_4 + PO_4$	16.07	15.5

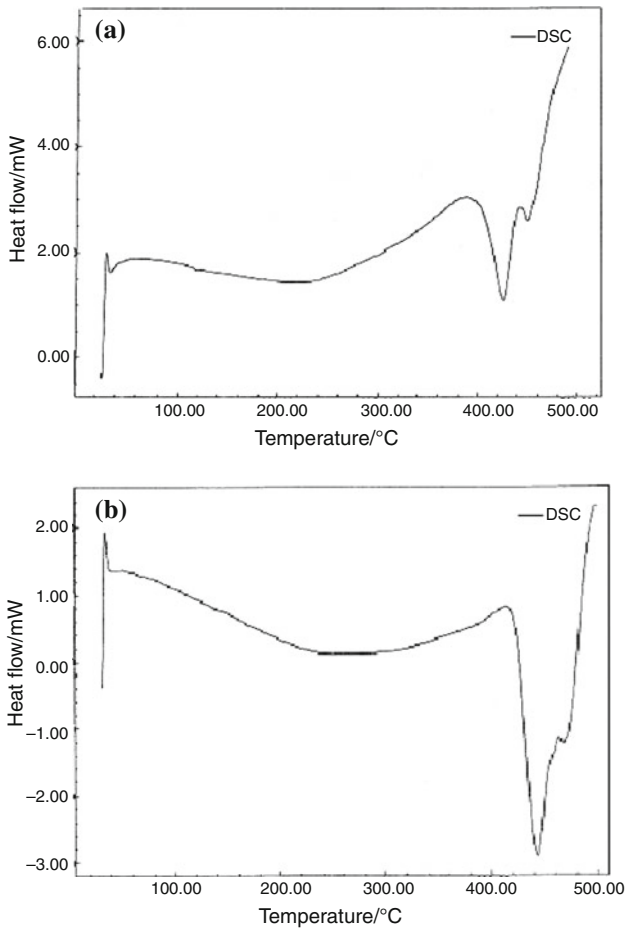

Fig. 8 Differential scanning calorimetry (DSC) plot depicting various endothermic and exothermic peaks for **a** BP; **b** CdBP

On application of the Horowitz–Metzger relation a good linear fit is observed for log [g (α)] against θ, where, g (α) = [1−(1−α)$^{1-n}$/1−n] or 2[1(1−α)$^{1/2}$] for both BP and CdBP crystals, there by suggesting geometrical contraction models in which geometrical contracting cylindrical model as the appropriate one for the mechanism of decomposition. According to these models, nucleation occurs rapidly on the crystal surface. The rate of degradation is controlled by the resulting reaction interface, which progress toward the center of the crystal. Depending on crystal shape, different mathematical models have been derived. For any crystal particle the following relation is applicable:

$$r = r_o - kt$$

where r is the radius at time t, r_o is the radius at time t_o, and k is the reaction rate constant. If a solid particle has cylindrical or spherical/cubical shapes, the contracting cylinder (contacting area) or contracting sphere/cube (contracting volume) models can be derived, respectively. Dehydration of calcium oxalate monohydrate was shown to follow geometrical contraction models [31]. As the crystal belongs to orthorhombic system, so in all probability it is the contracting cylindrical model, which is the most appropriate one for the explanation of thermal decomposition.

Activation energy (E_a) can be calculated from the slope of straight line using the formula:

$$\text{Slope } (m) = E_a/2.303\,RT_m^2 \quad \text{Or}$$
$$E_a = m \times 2.303\,RT_m^2/\text{K J mol}^{-1}$$

The frequency factor (Z) can be calculated by using the formula: $Z = E/RT_m^2\beta \exp(E/RT_m)/\text{S}^{-1}$; where '$Z$' is the frequency factor and 'β' is the heating rate.The entropy (ΔS^*) can be calculated by using the formula:

$$Z = KTm/h \exp(\Delta S^*/R) \quad \text{Or}$$
$$(\Delta S^*) = R \exp(Z\,h/kT_m)/\text{J K}^{-1}\,\text{mol}^{-1}$$

where 'ΔS^*' is the entropy, 'k' is the Boltzman constant and 'h' is the Planks constant

Coats–Redfern relation

Coats–Redfern relation is given by the equation

$$\log[g(\alpha)]/T^2] = \log[-\ln(1-\alpha)/T^2]$$
$$= \log[ZR/\beta E_a(1-2RT/E_a)]$$
$$- E_a/2.303\,RT \quad \text{for } n = 1$$
$$\log[g(\alpha)]/T^2] = \log\left[1-(1-\alpha)^{1-n}/1-n\right]$$
$$= \log[ZR/\beta E_a(1-2RT/E_a) - E_a]/$$
$$2.303\,RT \quad \text{for } n \neq 1$$

Here α, β, T, R, Z, and E are the same quantities as discussed in H–M relation. The plot of log [g (α)]/T^2] against 1/T yields a straight line for order of reaction n = ½. For n = ½ which turns out to be the best linear fit, g (α) = 2[1(1−α)$^{1/2}$] again suggesting contracting cylindrical model as the appropriate model for the decomposition of both BP and CdBP crystals. The plot of log [g (α)]/T^2] against 1/T yields a straight line, the slope of which ($m = -E_a/2.303\ R$) gives activation energy (E_a) ($E_a = -m \times 2.303\ R$)/K J mol^{-1}.

The frequency factor (Z) can be calculated from the intercept by using the formula:

$$C = \log ZR/\beta E_a \quad \text{or} \quad ZR/\beta E_a = 10^C; \quad \text{or}$$
$$Z = \beta E_a(10^C)/R/\text{S}^{-1}$$

The entropy (ΔS^*) can be calculated by using the formula:

$$(\Delta S^*) = R \exp(Z\,h/kT_m)/\text{ J K}^{-1}\,\text{mol}^{-1}$$

Table 5 Various kinetic parameters calculated from the thermogravimetric analysis using three different relations for both the crystals

TG method	Stage	Order of reaction n		Activation energy/K J mol^{-1}		Frequency factor Z/s^{-1}		Entropy (ΔS^*)/J K^{-1} mol^{-1}	
		BP	CdBP	BP	CdBP	BP	CdBP	BP	CdBP
Horowitz–Metzger	I	½	½	2.68	4.69	9.36	2.63×10^3	−212.65	−165.01
	II	½	½	77.16	29.05	2.02×10^7	3.52×10^1	−108.40	−217.88
Coats–Redfern	I	½	½	0.268	0.37	9.71×10^1	1.79×10^2	−193.25	−187.57
	II	½	½	0.12	0. 65	3.02×10^4	5.11×10^{-2}	−162.35	−272.25
Piloyan–Novikova	I	–	–	0. 35	0.409	2.9×10^{-3}	1.34×10^2	−367.94	−189.81
	II	–	–	0.033	0.054	9.2×10^{-4}	4.6×10^{-2}	−242.02	−273.92

Piloyan–Novikova relation

Piloyan–Novikova relation is:

$$\log\left[g(\alpha)/T^2\right] = \log\left[(\alpha)/T^2\right] = \log[ZR/\beta E_a - E_a/2.303\,RT]$$

where $\alpha = 0.04$–0.5, β is the heating rate at which temperature increases and Z is the frequency factor. This relation does not give the value of order of reaction and hence any modeling for decomposition. However, one can calculate the value of activation energy (E_a) from the slope and frequency factor (Z) from the intercept of straight line of the graph between log [$(\alpha)/T^2$] and $1/T$, respectively, as already explained for Coats–Redfern relation.

Table 5 gives compiled data for various kinetic parameters on applying the equations of Horowitz–Metzger, Coat–Redfern, and Piloyan–Novikova for both BP and CdBP crystals for two stages of thermal decomposition. From the results obtained on the solid-state reaction kinetic studies, the authors conclude that entropy in case of pure (BP) crystals is minimum for second stage of decomposition where as in case of doped (CdBP) crystals; entropy is minimum for first stage of decomposition. This means that in pure crystals second stage is more ordered than fist stage and in doped crystals the result is vice versa.

Conclusions

Based on the results, the following conclusions can be drawn:

- The growth of BP and CdBP crystals having formula $Ba_3(PO_4)_2{\cdot}H_2O$ and $Cd_{3(0.1)}Ba_{3(0.9)}(PO_4)_2{\cdot}H_2O$, respectively, is accomplished by employing room temperature solution technique, i.e., gel technique.
- BP and CdBP both belong to orthorhombic crystal system. The lattice parameters obtained in case of pure are: a = 4.60, b = 14.10, c = 17.16 Å and $\alpha = 90.00°$, $\beta = 90.02$, $\gamma = 90.00°$. Similarly, the lattice parameters obtained in case of doped crystals are: a = 4.59, b = 14.05, c = 17.10 Å and $\alpha = 90°$, $\beta = 90.01°$, $\gamma = 90.15°$. Thus, the crystal structure of BP remains unaffected by up to 30% doping of its composition.
- FTIR results support the presence of water of hydration and other functional groups in both pure and doped BP crystals.
- The qualitative and quantitative elemental analysis employing the EDAX technique, confirm the presence of major elements present in the grown crystal. The stoichiometric compositions of the grown crystals as established by EDAX technique is $Ba_3(PO_4)_2{\cdot}H_2O$ and $Cd_{3(0.1)}Ba_{3(0.9)}(PO_4)_2{\cdot}H_2O$.
- The thermal studies suggest that the pure crystal is stable up to temperature of 330 °C whereas doped crystal is stable up to a temperature of 240 °C. This means that doping of Cd in pure crystals decreases their thermal stability. Also the temperature for the formation of end product increases with Cd substitution.
- Among all the three relations used for studying non-isothermal kinetic parameters of thermal analysis, best linear fit is obtained by taking g $(\alpha) = 2[1(1-\alpha)^{1/2}]$ for different stages of decomposition of both the crystals. Thus, the model proposed for the thermal decomposition of the material is contracting cylindrical model.
- In pure crystals entropy is minimum for second stage of decomposition, which means that second stage is the more ordered stage.

Acknowledgements Authors are thankful to Prof. Rajnikant for carrying out single crystal X-ray studies using Single Crystal Oxford X-ray Diffractometer, sanctioned as National Facility by DST, India to the Department of Physics, University of Jammu.

References

1. Dinamani M, Kamath PV. Electrochemical synthesis of metal phosphates by cathodic reduction. Mat Res Bull. 2001;36:2043–50.
2. Sales BC, Chokousmakos BC, Boatner LA, Ramney JO. Structural investigation of the amorphous phases produced by heating crystalline MgHPO4.3H2O. J Cryst Sol. 1993;159:121–39.
3. Zaitseva N, Carman L. Rapid growth of KDP type crystals. Progr Cryst Growth Character Mater. 2001;43:1–118.

4. Devries SA, Goedtkindt P, Huisman WJ, Zwanenburg MJ, Feidenhans R, Bennett SL, Smilgus DM, Stierle A, De Yoreo JJ, Van Enckevort WJP, Bennema P, Vlieg E. X-Ray diffraction studies of potassium dihydrogen phosphate (KDP) crystal surfaces. J Cryst Growth. 1999;205:202–14.
5. Henisch HK. Crystal Growth in Gels. New York: Dover; 1996.
6. Blank Z, Speyer DM, Brenner W, Okomoto Y. Growth of single crystals of silver halides in silica gel at near ambient temperature. Nature. 1967;216:1103.
7. Barta C, Zemlicka J, Rene V. Growth of $CaCO_3$ and $CaSO_4.2H_2O$ crystals in gels. J Cryst Growth. 1971;10:158–62.
8. Koelmans H, Cox APM. Luminescence of modified Tin-activated strontium orthophosphate. J Electro Chem Soc. 1957;104:442–5.
9. Dishovshy N, Bonchev-Mladenova Z. Doping of gel grown Ag_2SeO_4 single crystal. J Cryst Growth. 1981;51:147–8.
10. Dennis J, Henisch HK. Nucleation and growth of crystals in gels. J Electro Chem Soc. 1967;114:263–6.
11. Gits S, Robert MC, Lefaucheux L. Doping effect on the crystalline quality of ADP doped chromium: 1. Composition of solution grown and gel grown crystals. J Cryst Growth. 1985;71:203–8.
12. Kanchana G, Suresh P, Sundaramoorthi P, Kalainathan S, Jeyanthi GP. Growth of strontium chromium magnesium hydrogen phosphate (SrCrMHP) crystals in silica gel medium at different growth environments and nucleation reduction strategy. J Mineral Mater Character Eng. 2008;7:215–31.
13. Kanchana G, Sundaramoorthi P, Jeyanthi G. P. Growth and characterization studies of strontium calcium magnesium hydrogen phosphate (SrCaMHP) crystals in silica gel medium and laser induced nucleation reduction strategy. J Mineral Mater Character Eng. 2009;8:37–45.
14. Jaw KS. Preparation of a biphasic calcium phosphate from $Ca(H_2PO_4)_2\,2H_2O$ and $CaCO_3$. J Therm Anal Calorim. 2006;83:145.
15. Madhurambal G, Subha R, Mojumdar SC. Crystallization and thermal characterization of calcium hydrogen phosphate dihydrate crystals. J Therm Anal Calorim. 2009;96:73–6.
16. Samuel VM, Unikrishnan NV, Ittyachen MA. Thermal characterization of pure and neodymium doped calcium hydrogen phosphate single crystals. J Therm Anal Calorim. 2009;96:917–21.
17. Varshney KG, Agrawal A, Mojumdar SC. Pyridine based thorium (iv) phosphate hybrid fibrous ion exchanger synthesis, characterization and thermal behaviour. J Therm Anal Calorim. 2007; 90:721–4.
18. Varshney KG, Agrawal A, Mojumdar SC. Pyridine based cerium (iv) phosphate hybrid fibrous ion exchanger synthesis, characterization and thermal behaviour. J Therm Anal Calorim. 2007;90:731–4.
19. Rathore HS, Varshney G, Mojumdar SC, Saleh MT. Synthesis, characterization and fungicidal activity of zinc diethyldithiocarbonate and phosphate. J Therm Anal Calorim. 2007;90:681–6.
20. Varshney KG, Agrawal A, Mojumdar SC. Pectin based cerium (iv) and thorium (iv) phosphates as novel hybrid fibrous ion exchangers synthesis, characterization and thermal behaviour. J Therm Anal Calorim. 2005;81:183–9.
21. Kanchana G, Sundaramoorthi P. In vitro studies of calcium mixed minerals growth in different growth faces and semiconductor laser induced suppression of nuclei and strategy. Bull Mater Sci. 2008;31:981–5.
22. Sundaramoorthi P, Kanchana G, Kalainathan S. Laser irradiation of $BaMgHPO_4$ crystals in silica gel media at different growth environments (nucleation reduction strategy) and its characterization studies. Spectrochemi Acta A. 2008;69:1154–9.
23. Hebber KC, Dharma Prakash SM, Mohan Rao P. Physico–chemical characterization of BaHPO4. Bull Mater Sci. 1991;14: 1219–23.
24. Pan DY, Yuan DR, Sun HQ, Guo SY, Wang XQ, Duan XL, Luan CN, Li ZF. Solubility and crystallization of $BaHPO_4$ crystals. Cryst Res Technol. 2006;41:236–8.
25. Sundaramoorthi P, Kalainathan S. Crystal growth of some renal stones constituents: I. In vitro crystallization of trace elements and its characterization studies. J Mineral Mater Character Eng. 2007;6:17–24.
26. Joshi SJ, Parekh BB, Vohra KD, Joshi MJ. Growth and characterization of gel grown pure and mixed levo–tartrate crystals. Bull Mater Sci. 2006;29:307–12.
27. Sestak J. Thermal analysis. In: H. G. Wiedemann (ed) Proceedings of the third international conference on thermal analysis, 1971; 2:24.
28. Horowitz HH, Metzger G. A new analysis of thermogravimetric traces. Anal Chem. 1963;35:1464–8.
29. Coats AW, Redfern JP. Kinetic parameters from thermogravimetric data. Nature. 1964;201:68.
30. Piloyan GO, Ryabchikov ID, Novikova OS. Determination of activation energies of chemical reactions by differential thermal analysis. Nature. 1966;212:1229.
31. Gao ZM, Amasaki I, Nakada M. A description of kinetics of thermal decomposition of calcium oxalate monohydrate by means of the accommodated Rn model. Thermochim Acta. 2002;385:95–103.